

Use of Simulated Annealing Technique for Finding Most Bound Structures in Nuclear Reactions

Samiksha Sood¹, Ishita Puri², Rohit Kumar³, Arun Sharma⁴ and Rajeev K. Puri¹

Abstract—Using quantum molecular dynamics (QMD) model as phase space generator and energy based clusterization algorithm namely simulated annealing clusterization algorithm (SACA), we study the role of temperature of nuclear system on the final cluster structures by implementing different thermal binding energies in the computer analysis code. We find that the inclusion of different thermal binding energies do not affect the final observations significantly. We also compare our calculations with experimental data and find consistent results.

Index Terms—Molecular dynamics model, clusterization algorithm, heavy-ion collisions at intermediate energies, computer clusterization code.

I. INTRODUCTION

At intermediate energies, heavy ion collisions may be conjectured as a sequence of different physical conditions [1-4]. Well before the collision, projectile and target are in their respective ground states. As soon as they touch each other, they form a compressed and highly excited unstable system. The kinetic energy stored in the system in the form of pressure gradient causes the expansion of this unstable system that shatters into number of excited clusters. With the passage of time, these clusters move away from each other and get de-excited by emitting particles. To develop the theory which explains this compression-expansion scenario is a very tedious task in the present era [4-15]. On one hand, it has been considered that the disassembly of nuclear matter into clusters have statistical (thermal) origin [4, 5], whereas on the other hand, dynamical picture of fragment origin is also found to be equally successful [5, 6]. As the statistical models cannot follow the time evolution of clusters, therefore, dynamical models are more suitable for this purpose. In the present study, we will discuss cluster formation in heavy-ion collisions by considering dynamical picture of fragment formation in the light of many-body dynamical models [5,6].

Every dynamical model provides information of the colliding system in form of time evolution of the phase space of nucleons. As these models do not provide cluster information directly, therefore, the phase space of nucleons is injected into secondary clusterization algorithms [5,6]. Among different clusterization algorithms (that vary from checking

simple spatial constraints between the nucleons to the complex energy based algorithms [5-15]); we will use simulated annealing clusterization algorithm (SACA) in the present study [13]. This clusterization algorithm is based on the energy minimization that can find the fragment structures at the earlier times when nucleonic matter is still in interaction phase (approximately 60-100 fm/c). Its early versions ignored the excitation energy or the temperature of the fragmenting system while searching for the most bound structure.

In the literature, many efforts have been devoted to find the temperature of the fragmenting system [16-20]. Different thermometers are introduced, which use different properties of the fragmenting system to measure the temperature attained by the fragmenting system. One of the first methods to measure the temperature of the compressed system has been introduced by Albergo *et al* [19], which took the base line from the Hoyle *et al* [20]. They used the ratio of the isotopes of light fragments formed in the reactions. Further, there are other thermometers based on the isotope ratios of heavy fragments, kinetic energy spectra of the light fragments etc. In all these studies, it was observed that the temperature of the fragmenting system comes out to be upto 6 MeV [16-18].

It is worth mentioning that in the recent times, spatial clusterization algorithm has been improved by including temperature of the system [12]. Motivating from this study, in the present work, we will extend the SACA computer code by including the temperature of the system in the numerical formulation in the terms of temperature-dependent binding energies. It is worth mentioning that the studies of Karthikraj *et al* [21] at low incident energies and Souza *et al* [22] at intermediate energies, showed significant effect of different binding energies on various observables and non-observables. The present study will be extended in this direction by using different forms of the temperature-dependent binding energy formulae in the SACA formulation. We will particularly use the formulae devised by Davidson *et al* [23], Pi *et al* [24] and Sauer *et al* [25]. We will also compare our results with the experimental observations.

In section II, we will give brief description of the primary model QMD. Then, we will give brief details of the SACA and different temperature-dependent binding energy formulae used in section III. Section IV will deal with the comparison of our results with the available experimental data. Lastly, we will summarize our work in section V.

II. QUANTUM MOLECULAR DYNAMICS MODEL

Due to complicated physics involved in the breakup process, a complex model with auxiliary tools is needed. The initial information of the time evolution of the collision is

¹Department of Physics, Panjab University, Chandigarh-160014. (corresponding author e-mail: rkpuri@gmail.com).

²Department of Information Technology, UIET, Panjab University, Chandigarh-160014.

³Department of Physics, Dayanand Anglo-Vedic College, Chandigarh -160 010.

⁴G. D. College, Thanna Mandi, Rajouri, Jammu and Kashmir-185212.

modeled with quantum molecular dynamics (QMD) computer program [6]. The QMD model is an n-body dynamical model that operates at nucleonic level. In this model, each nucleon is represented by a Gaussian wave packet in coordinate and momentum space. The time evolution of the centroid of nucleonic wave packet is obtained by using classical Hamilton's equations of motion:

$$\frac{d\vec{r}_i}{dt} = \frac{d\langle H \rangle}{d\vec{p}_i}; \frac{d\vec{p}_i}{dt} = -\frac{d\langle H \rangle}{d\vec{r}_i},$$

(1)

here the Hamiltonian ($\langle H \rangle$) is the sum of the kinetic energy ($\langle T \rangle$) and potential energy ($\langle V \rangle$) of the n-body system

$$\langle H \rangle = \langle T \rangle + \langle V \rangle.$$

Here $\langle V \rangle$ consists of contributions from phenomenological Skyrme, long range Yukawa and Coulomb interactions. During the propagation, two nucleons are assumed to suffer collisions if the distance between their centroids is less than

$$\sqrt{\frac{\sigma(\sqrt{s})}{\pi}},$$

(2)

where $\sigma(\sqrt{s})$ is the total cross-section depending on the invariant mass \sqrt{s} . The phase space thus generated is stored at number of time steps and is injected into clusterization algorithm/computer code to obtain cluster information.

III. SIMULATED ANNEALING CLUSTERIZATION ALGORITHM (SACA): EXTENDED COMPUTER CODE

This robust clusterization algorithm is based on the principle of energy minimization of fragmenting system. This algorithm can realize the final fragment structures very early in time, therefore, valuable information about the fragment formation, space and velocity co-relations can be studied at all times, especially at the early stages of the reaction. In this algorithm at the initial stage, one starts from a random configuration, from which, all possible cluster configurations are constructed by shifting single nucleons or clusters from one cluster identity to other cluster. All these possible configurations are stored at all times. At final times, only that cluster configuration will be realized for which the fragmenting system has most bound structure.

In order to avoid the formation of unrealistic clusters at intermediate steps of the SACA technique, the binding energy of each cluster (ζ_i) is checked according to the following condition:

$$\zeta_i = \sum_{\alpha=1}^{A_f} \left[\sqrt{(p_\alpha - P_{A_f}^{cm})^2 + m_\alpha^2} - m_\alpha + \frac{1}{2} \sum_{\beta \neq \alpha}^{A_f} V_{\alpha\beta}(x_\alpha, x_\beta) \right] < E_{bind}^{therm} \times A_f,$$

(3)

where E_{bind}^{therm} is the temperature-dependent binding energy defined in the following paragraph. In the above equation, A_f is the number of nucleons part of a cluster and $P_{A_f}^{cm}$ is the center-of-mass momentum of that cluster. The temperature-dependent binding energies E_{bind}^{therm} are calculated using temperature-dependent binding energy formulae of Davidson *et al*, Pi *et al* and Sauer *et al*. Let us discuss these binding energy formulae briefly.

A. Temperature-dependent binding energy formulae

Sauer *et al* [25] formulated the temperature dependence of binding energies on the foundation of thermal Hartree-Fock approximation (THFA). In the THFA theory, the effect of temperature on the structure of the nuclei is also included in the calculations. In this theory, the energy per particle for infinite nuclear matter (i.e., volume energy + volume symmetry energy term) is obtained by using Skyrme force parameters in Hartree-Fock calculations. The energy for finite nuclei is calculated by using temperature-dependent Hartree-Fock theory. Then subtracting these two energies one can obtain the surface, free surface and Coulomb energy contributions for finite nucleus. The formula in its final form is written as:

$$E_{bind}^{Sauer}(T) = (-16.1 + 0.055T^2)A_f + (19.0 + 0.15T^2)A_f^{2/3} + 0.7(1.0 - 10^{-3}T^2)\frac{Z_f^2}{A_f^{1/3}} + 30.02(1.0 + 2.0 \times 10^{-4}T^2)\frac{(A_f - 2Z_f)^2}{A_f}.$$

(4)

In this formula, Z_f is the charge and A_f is the mass number of the cluster. On the other hand, Pi *et al* [24] used finite-temperature nuclear Thomas-Fermi model. In this theory, the nuclear density varies continuously from centre to exterior, dissimilar to the Sauer *et al* [25]. The formula in the final form reads as:

$$E_{bind}^{Pi}(T) = (a_v + \alpha_v T^2)A_f + (a_s + \alpha_s T^2)A_f^{2/3} - \left[\frac{3e^2}{5r_0} \left(1 - \frac{a_{Coul}}{A_f^{2/3}} \right) + \alpha_{Coul} T^2 \right] \frac{Z_f^2}{A_f^{1/3}} + (a_{sym} + \alpha_{sym} T^2) \frac{(A_f - 2Z_f)^2}{A_f} + (a_{ss} + \alpha_{ss} T^2) \frac{(A_f - 2Z_f)^2}{A_f^{4/3}}.$$

(5)

The parameters used in the above formula are given in Ref. [24].

The third formula used in the present study is parameterized by Davidson *et al* [23] in the framework of canonical ensemble theory. This formula takes care of the pairing energy also and reads as:

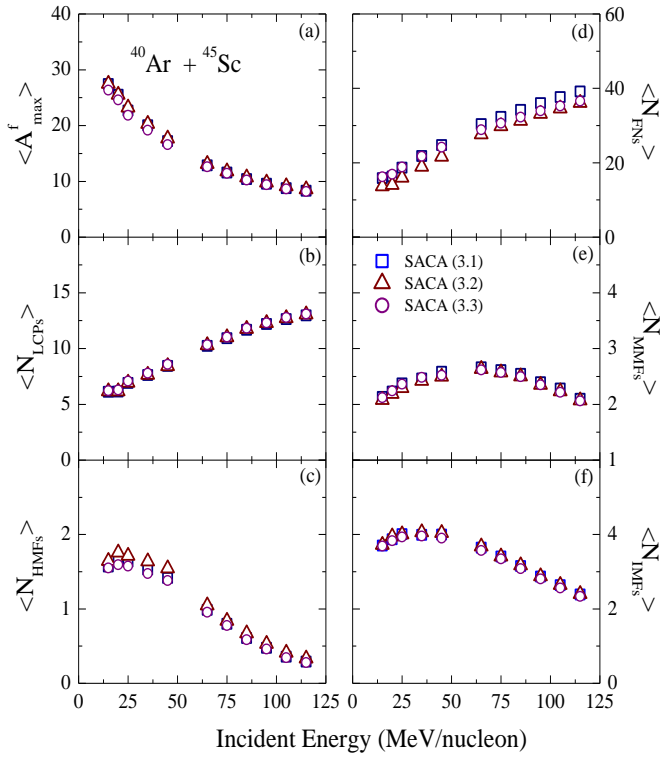


Fig.1. The mean size of the largest fragment $\langle A_{\max}^f \rangle$ and multiplicities of the free nucleons (FNs), LCPs, MMFs, HMFs and IMFs for the central reactions of $^{40}\text{Ar} + ^{45}\text{Sc}$ as a function of incident energy.

$$E_{\text{bind}}^{\text{Davidson}}(T) = \alpha(T)A_f + \beta(T)A_f^{2/3} + \left(\gamma(T) - \frac{\eta(T)}{A_f^{1/3}} \right) \frac{(4t_\zeta^2 + 4|t_\zeta|)}{A_f} + 0.8706 \frac{Z_f^2 R(0)}{A_f^{1/3} R(T)} \left(1 - \frac{0.7636}{Z_f^{2/3}} - 2.29 \frac{R(0)^2}{[R(T)A_f^{1/3}]^2} \right) + \delta(T) \frac{f(A_f, Z_f)}{A_f^{3/4}} \quad (6)$$

The values of the parameters used in the above formula are extracted from the graphs in Ref. [23].

The earlier SACA computer code was extended by incorporating the above binding energy formulae in the simulations. Due to these extensions, the computation time further increases many folds. Currently, we are working to upgrade the computer code to minimize the computation time. The SACA versions with temperature-dependent binding energy cut of Davidson *et al*, Pi *et al*, and Sauer *et al* are labeled as SACA (3.1), SACA (3.2) and SACA (3.3), respectively.

IV. RESULTS AND DISCUSSION

In Fig. 1, we display the incident energy dependence of the mean size of the largest fragment ($\langle A_{\max}^f \rangle$) and multiplicities of the free nucleons (FNs), light charged particles (LCPs) [$2 \leq A_f \leq 4$], medium mass fragments (MMFs) [$5 \leq A_f \leq 9$], heavy mass fragments (HMFs) [$10 \leq A_f \leq 28$] and intermediate mass fragments (IMFs) [$5 \leq A_f \leq 28$] for the central reactions of $^{40}\text{Ar} + ^{45}\text{Sc}$. The squares, triangles and circles represent the results obtained using SACA (3.1), SACA (3.2) and SACA

(3.3), respectively. All results are at time of minimum in $\langle A_{\max}^f \rangle$.

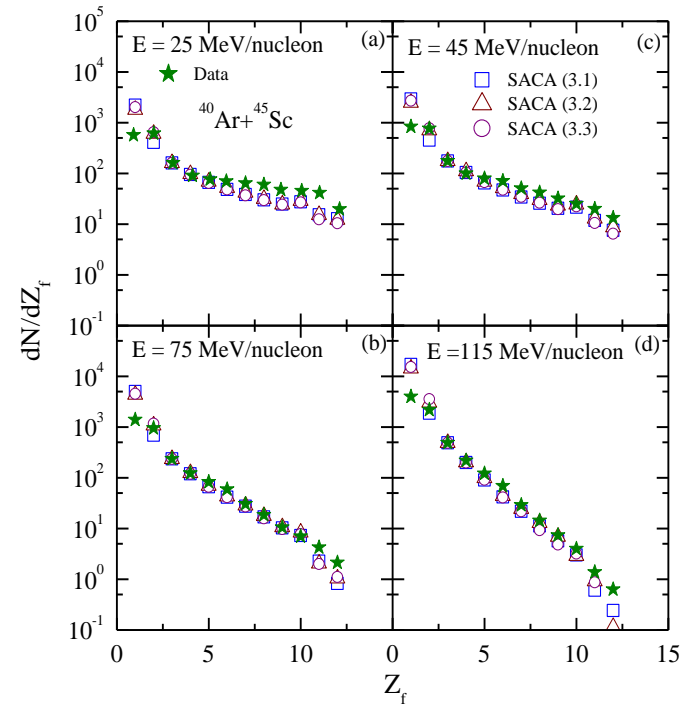


Fig.2. The charge distribution of the central reactions of $^{40}\text{Ar} + ^{45}\text{Sc}$ at incident energies of 25, 45, 75 and 115 MeV/nucleon. The experimental data [26] is shown by stars and other symbols are described in the text.

From the figure, we see that with the increase in the projectile incident energy, the mean size of the largest fragment decreases ($\langle A_{\max}^f \rangle$) and multiplicity values of free nucleons and LCPs increases continuously. On the other hand, the multiplicities of MMFs, HMFs and IMFs show a rise and fall behavior. These different behaviors of different clusters as a function of the projectile incident energy can be understood as following:

At lower incident energies, lesser energy is stored in the system; hence, nuclear system will have a large single fragment and lesser number of other fragments. As the projectile incident energy increases, more energy is deposited in the colliding system that will produce more breaking in the system. Due to which the mean size of the largest fragment decreases and the multiplicity of all cluster sizes increases. If the projectile incident energy is further increased, the possibility to obtain bound cluster decreases. Therefore, we see a rise and fall behavior for MMFs, HMFs and IMFs. The value of the energy at which maximum clusters are produced shifts to higher values as one goes from HMFs to IMFs to MMFs. The free nucleons and LCPs have contribution from lighter masses, therefore, the peak in the multiplicity will be observed at much higher energies than considered in the present study. Also note that, multiplicities of free nucleons and LCPs have two types of contributions: first at the pre-equilibrium stage of the reaction and second due to the evaporation from the excited heavier fragments. Therefore, things get mixed up and we cannot depict the exact behavior,

we can only conjecture the rising behavior in the multiplicities of the free nucleons and LCPs.

From the figure, we also see that the role of including temperature-dependent binding energies in the analysis is very small and do not influence the final results significantly. One can see that all versions of SACA computer modeling show similar behavior for all the fragment masses and also give same absolute values. These results indicate that the SACA computer algorithm is independent of the binding energy cut. Of course, if cold binding energies are implemented then one may get difference as clusters are not be cold, but excited.

V. COMPARISON OF OUR THEORETICAL RESULTS WITH EXPERIMENTAL DATA

It may happened that total multiplicity values come out to be same with all versions of SACA computer modeling but individual fragment structure that lies in the same mass windows may change. To deal with this aspect, we present the comparison of our theoretical results obtained using different versions of SACA computer code for multiplicity values of individual fragments in terms of charge distribution of the fragments. We will also compare our calculations using various versions of SACA algorithm with the available experimental data to ensure that SACA includes the relevant physics.

In the Fig. 2, we display the charge distribution for the central reactions of $^{40}\text{Ar} + ^{45}\text{Sc}$ at incident energies of 25, 45, 75 and 115 MeV/nucleon. The experimental data points [26] are represented by the stars and other symbols have the same meaning as that in Fig.1. Calculated results are normalized to experimental data at $Z_f = 3$. From the figure, we see that the slope of the charge distribution becomes steeper as the incident energy is increased. This happen due to the reason that with increase in the energy, the deposited incident energy increases and more number of lighter particles will sustain after the reaction as compared to heavier one. One can clearly see that the experimental trends and the absolute yields are reasonably reproduced by all versions of SACA computer codes using different formulae for analysis.

VI. SUMMARY

In this work, we have tested the sensitivity of the energy based algorithm SACA towards the inclusion of temperature of the fragmenting system. For this, clusterization/computational algorithm was extended to include temperature-dependent binding energies. Our calculations demonstrate nearly insensitive response towards different binding energies. As computational time increases many fold, currently we are working to upgrade computer code to have faster outcome.

REFERENCES

- [1] M. B. Tsang *et al.*, "Onset of Nuclear Vaporization in $^{197}\text{Au} + ^{197}\text{Au}$ Collisions", Phys. Rev. Lett. **71**, 1502 (1993).
- [2] A. Schuttauf *et al.*, "Universality of spectator fragmentation at relativistic bombarding energies", Nucl. Phys. A **607**, 457 (1996).
- [3] W. Bauer, G. F. Bertsch, W. Cassing and U. Mosel, "Energetic photons from intermediate energy proton- and heavy-ion-induced reactions", Phys. Rev. C **34**, 2127 (1986).
- [4] G. F. Peaslee *et al.*, "Energy dependence of multifragmentation in $^{84}\text{Kr} + ^{197}\text{Au}$ collisions", Phys. Rev. C **49**, R2271 (1994).
- [5] B. Borderie and M. F. Rivet, "Nuclear multifragmentation and phase transition for hot nuclei", Prog. Part. and Nucl. Phys. **51**, 551 (2008).
- [6] J. Aichelin, "Quantum molecular dynamics: A dynamical microscopic *n*-body approach to investigate fragment formation and the nuclear equation of state in heavy-ion collisions", Phys. Rep. **202**, 233 (1991).
- [7] S. Kumar and R. K. Puri, "Role of momentum correlations in fragment formation" Phys. Rev. C **58**, 320 (1998).
- [8] C. Dorso and J. Randrup, "Early recognition of clusters in molecular dynamics model", Phys. Lett. B **301**, 328 (1993).
- [9] J. Singh and R. K. Puri, "Study of the formation of fragments with different clusterization methods" J. Phys. G: Nucl. Part. Phys. **27**, 2091 (2001).
- [10] S. Kumar and R. K. Puri, "Stability of fragments formed in the simulations of central heavy ion collisions" Phys. Rev. C **58**, 2858 (1998).
- [11] S. Goyal and R. K. Puri, "Formation of fragments in heavy-ion collisions using a modified clusterization method", Phys. Rev. C **83**, 047601 (2011).
- [12] R. Kumar, S. Gautam and R. K. Puri, "Multifragmentation within a clusterization algorithm based on thermal binding energies", Phys. Rev. C **89**, 064608 (2014).
- [13] R. K. Puri and J. Aichelin, "Simulating annealing clusterization algorithm for studying the multifragmentation", J. Comput. Phys. **162**, 245 (2000).
- [14] Y. K. Vermani and R. K. Puri, "Microscopic approach to the spectator matter fragmentation from 400 to 1000 MeV/nucleon", Euro. Phys. Lett. **85**, 62001 (2009).
- [15] A. Le Fevre, Y. Leifels, J. Aichelin, C. Hartnack, V. Kireyev and E. Bratkovskaya, "FRIGA, a new approach to identify isotopes and hypernuclei in *n*-body transport models", J. Phys.: Conf. Ser. **668**, 012021 (2016).
- [16] J. B. Natowitz *et al.*, "Caloric curves and critical behavior in nuclei", Phys. Rev. C **65**, 034618 (2002).
- [17] J. Wang *et al.*, "Tracing the evolution of temperature in near Fermi energy heavy ion collisions", Phys. Rev. C **72**, 024603 (2005).
- [18] A. Barranon, C. O. Dorso and J. A. Lopez, "Time dependence of isotopic temperatures", Nucl. Phys. A **791**, 222 (2007).
- [19] S. Albergo, S. Costa, E. Costanzo and A. Rubbino, "Temperature and free-nucleon densities of nuclear matter exploding into light clusters in heavy-ion collisions", Nuovo Cimento A **89**, 1 (1985).
- [20] F. Hoyle, "The synthesis of elements from hydrogen, Monthly Notices of the Royle Astronomy", Soc. **106**, 343 (1946).
- [21] C. Karthikraj *et al.*, "Temperature-dependent binding energies in a dynamical cluster-decay model applied to the decay of hot and rotating $^{56}\text{Ni}^{*}$ ", Phys. Rev. C **86**, 014613 (2012).
- [22] S. R. Souza *et al.*, "Probing the symmetry energy from the nuclear isoscaling", Phys. Rev. C **78**, 014605 (2008).
- [23] N. J. Davidson *et al.*, "A semi-empirical determination of the properties of nuclear matter", Phys. Lett. B **315**, 12 (1993).
- [24] M. Pi, X. Vinas and M. Barranco, "Estimation of temperature effects on fission barriers", Phys. Lett. B **26**, 733 (1982).
- [25] G. Sauer, H. Chandra and U. Mosel, "Thermal properties of nuclei", Nucl. Phys. A **264**, 221 (1976).
- [26] T. Li *et al.*, "Intermediate Mass Fragment Production in Central Collisions of Intermediate Energy Heavy Ions", Phys. Rev. Lett. **70**, 1924 (1993).